Grant Title: **3-D Coronal-Solar Wind Energetic Particle Acceleration (C-SWEPA) module**
1st Year Progress Report
PI: Nathan A. Schwadron
Period of performance: 3/25/2013 – 3/24/2014
University of New Hampshire
8 College Road, Durham, NH 03824
Grant Number: NNX13AI75G

TABLE OF CONTENTS

I. C-SWEPAObjectives:

The 3-D Coronal-Solar Wind Energetic Particle Acceleration (C-SWEPA) modules provide tools for taking the critical next step in understanding Solar Energetic Particle (SEP) events and characterizing their hazards through physics-based modeling *from the low corona through the inner heliosphere*. *C-SWEPA's central objective is to develop and validate a numerical framework of physics-based modules that couple the low corona and CMEs with solar wind, shocks, and particle acceleration.* Simulated observers (e.g., spacecraft near L1, Earth, moon, Mars, etc.) provide basis for comparison with spacecraft and tools to explore simulated mission datasets (e.g., Solar Probe Plus, SPP, and Solar Orbiter, SolO).

C-SWEPA fulfills the need for a transformative synthesis of LWS capabilities by bringing together an exceptional team of leading experts from five institutions in solar, heliospheric and magnetospheric physics and two successful LWS strategic capabilities: the Earth-Moon-Mars Radiation Environment Modules (EMMREM), and the Next Generation Model for the Corona and Solar Wind. C-SWEPA leverages new advancements in High Performance Computing (HPC) through the use of heterogeneous architectures (Graphical Processing Units; GPUs) and develops an innovative approach to delivering complex models that enables the CCMC to use dedicated GPU-enabled and massively parallelized systems for C-SWEPA simulations.

C-SWEPA is a transformational project providing: an integration between observationally-driven modeling of CMEs, solar wind, shocks and energetic particles from the low corona through the heliosphere; incorporation of seed populations and associated compositional dependencies; and detailed models that probe the steady and disturbed corona thus paving the way for SolO and SPP studies.

C-SWEPA deliverables include: two numerical systems (one at the CCMC and one at UNH) that run C-SWEPA; documentation; and an intuitive interface. These systems provide: on-line availability and event scenarios from Sun-to-Earth; runs that include solar wind, CMEs and associated shock(s), SEP flux time series, dose & dose-equivalent rates, integrated doses behind various layers of shielding; and results of runs made for specific campaign events of interest to the science community at large. Both EMMREM and CORHEL run at the CCMC and the associated teams have a strong history of partnering with the CCMC.

C-SWEPA answers fundamental scientific questions that study the corona, solar wind, CME initiation, shocks, solar energetic particle acceleration and propagation. Core team members have experience working together and leverage developments from CISM, EMMREM, CORHEL, NSF's FESD Sun-to-Ice project, and existing Focus Science Teams (FSTs) of NASA's Living With a Star (LWS) Program.

C-SWEPA provides broad impacts by advancing discovery and understanding while also promoting teaching, training of graduate students, undergraduate involvement, and participation of under-represented groups. C-SWEPA enhances the infrastructure for research and education through development of computing capabilities for the science community. By advancing tools for understanding and predicting space weather, C-SWEPA provides important societal benefits enabling expansion of space technologies.

Currently, C-SWEPA is completing its first milestone in procuring hardware and modeling a single event Sun-to-Earth.

II. C-SWEPA Accomplishments:

II.1 C-SWEPA Progress in Understanding of Protracted Minimum of Cycle 23/24 and the the Mini Maximum Cycle 24

The deep solar minimum between cycles 23 and 24 and the activity in cycle 24 differed significantly from those of the prior cycle (Schwadron et al., 2011; McComas et al., 2013). In the solar minimum, the fast wind was slightly slower, was significantly less dense and cooler, had lower mass and momentum fluxes (McComas et al., 2008), and weaker heliospheric magnetic fields (Smith et al., 2008). During the rise of activity in cycle 24 the mass flux of solar wind remained low, (McComas et al., 2013b) and the magnetic flux of the heliosphere remained at significantly lower levels than observed at previous solar maxima in the space age (Smith et al., 2013). (McComas et al.,, 2013b) showed that the current "mini" solar maximum of cycle 24 has shown only a small recovery in particle and magnetic fluxes. Therefore, the cycle 24 mini solar maximum continues to display the same trends as observed in the cycle 23-24 minimum. In fact, conditions during the cycle 23-24 minimum appear to be similar to conditions at the beginning of the 1800's at the start of the Dalton Minimum (Goelzer et al., 2013). Taken together, these recent changes suggest that the next solar minimum may continue to show declining sunspot numbers, associated with declining values of magnetic flux and further reductions in solar wind particle flux.

Using the model from Schwadron et al. (2010) and monthly average sunspot numbers, Goelzer et al. (2013) were able to compute a monthly average HMF intensity from 1749 to the present. For comparison, Goelzer et al (2013) looked at the work of McCracken (2007), who modeled the HMF intensity from the levels of paleogenic nucleotide ^{10}Be and the Omni2 data, which is available back to 1963. These three estimations of flux as well as sunspot number are shown in Figure 1, with a strong correlation and a clear hysteresis.

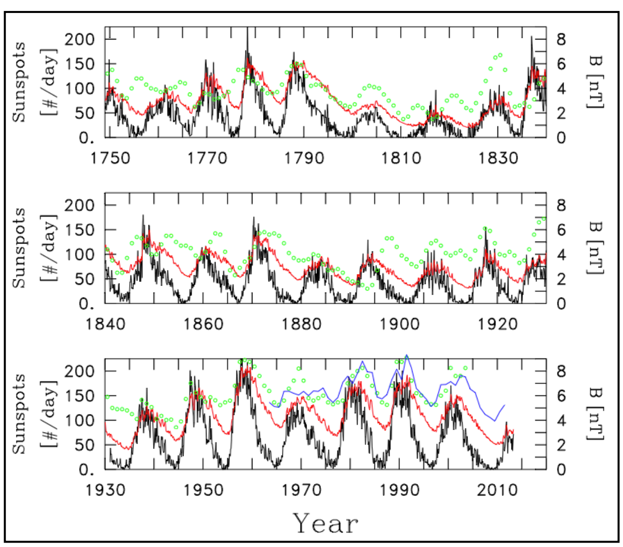

Figure 1: *(black) Monthly ave SSN. (red) Predicted Parker comp. of the HMF intensity. (green) Yearly ave HMF intensity derived from ^{10}Be data. (blue) Measured yearly aves of HMF intensity (Smith et al. [2013]) from the Omni2 data.*

The anomalously weak heliospheric magnetic field and low solar wind flux during the last solar minimum have resulted in galactic cosmic rays (GCRs) achieving the highest flux levels observed in the space age (Mewaldt et al., 2010), and fluxes continue to be unusually elevated through the cycle 24 maximum. It is unknown if the recent anomalous deep solar minimum hints at larger changes in the near future, or if the unusual changes in GCR fluxes and conditions on the Sun have an impact on Earth's atmosphere. Given the fact that GCR radiation can damage living tissue, causing cellular mutagenesis, the changing state of the Sun may have long-term implications for life on the planet. Figure 2 illustrates the critical growing record of dose rate throughout the LRO mission that quantifies the changing conditions and radiation hazards posed by GCRs and SEPs. Pronounced discrete SEP events punctuate the underlying trend of diminishing long-term GCR doses.

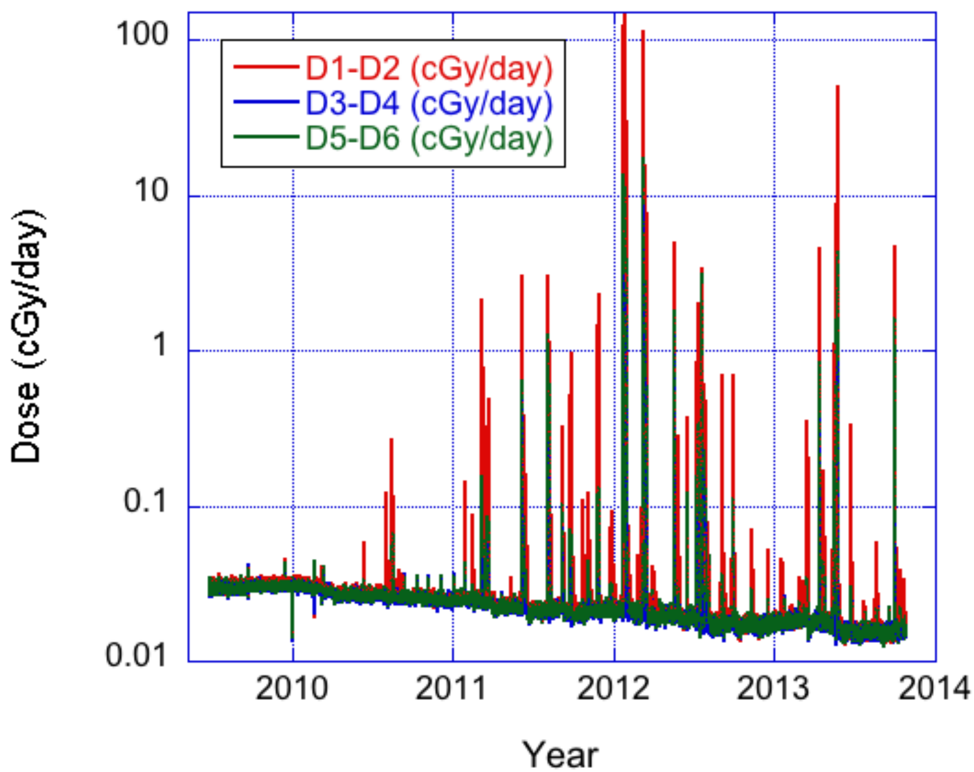

Figure 2. *Dose Rates over time through the quantify radiation hazards that damage tissue, materials, and chemically change materials such as lunar regolith.*

The extremely high energies of GCRs make them both relevant to biology on the Earth, and also one of the greatest hazards for long-term space exploration. In deep interplanetary space and away from the shielding of Earth's atmosphere and magnetic field, these high energy particles are difficult to shield against, as some particles surpass a billion electron volts of kinetic energy. The effects of GCRs on the Earth system, including the biosphere, remain poorly understood and are oftentimes highly controversial (Shaviv and Veizer, 2003); this is because GCRs not only present a hazard to life through the breakdown of DNA, but also may help to stimulate evolution by increasing the rate of cell mutation (Todd, 1994). For example, a recent study of global diversity from paleontological data suggests there is a significant cycle of approximately 62 million years over which biodiversity rises and then falls; this cycle as of yet has no agreed upon cause but may be driven by extraplanetary processes (Rohde and Muller, 2005).

Joyce et al. [2013a] used the modulation potential at the Moon in conjunction with C-SWEPA data products to calculate galactic cosmic ray (GCR) dose and dose equivalent rates in the Earth and Mars atmospheres for various altitudes since 2009. Our results generally conform to expectations and are in good agreement with CRaTER observations. The results therefore may be used as reasonable estimates for use in efforts in risk assessment in the planning of future space missions as well as in the study of GCRs.

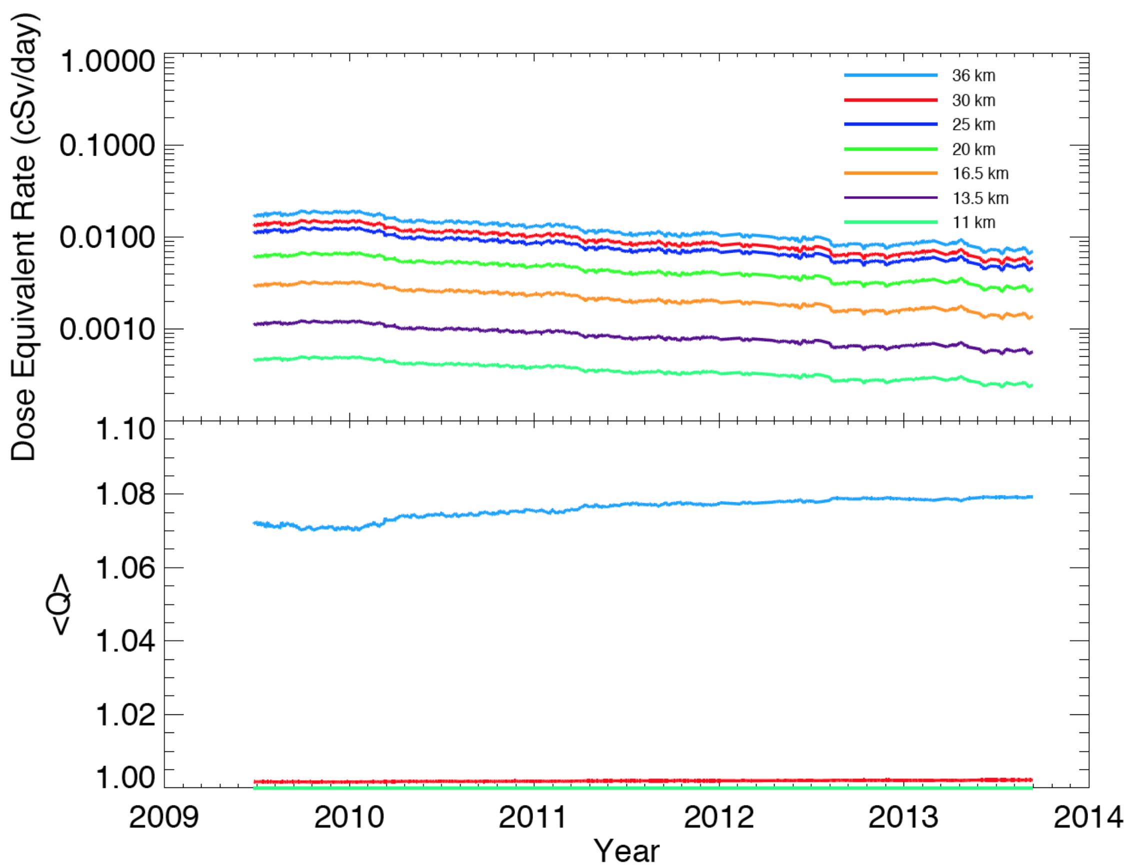

Figure 3. *Plot of the computed GCR dose equivalent rate for various altitudes in Earth's atmosphere since 2009.. Also shown is the ratio between the dose and dose equivalent rates, which gives the dose-weighted quality factor <Q>. We see that there is little to no difference between the dose and dose equivalent rates except for at the highest altitude where we see an approximate 7-8% increase relative to the dose rate.*

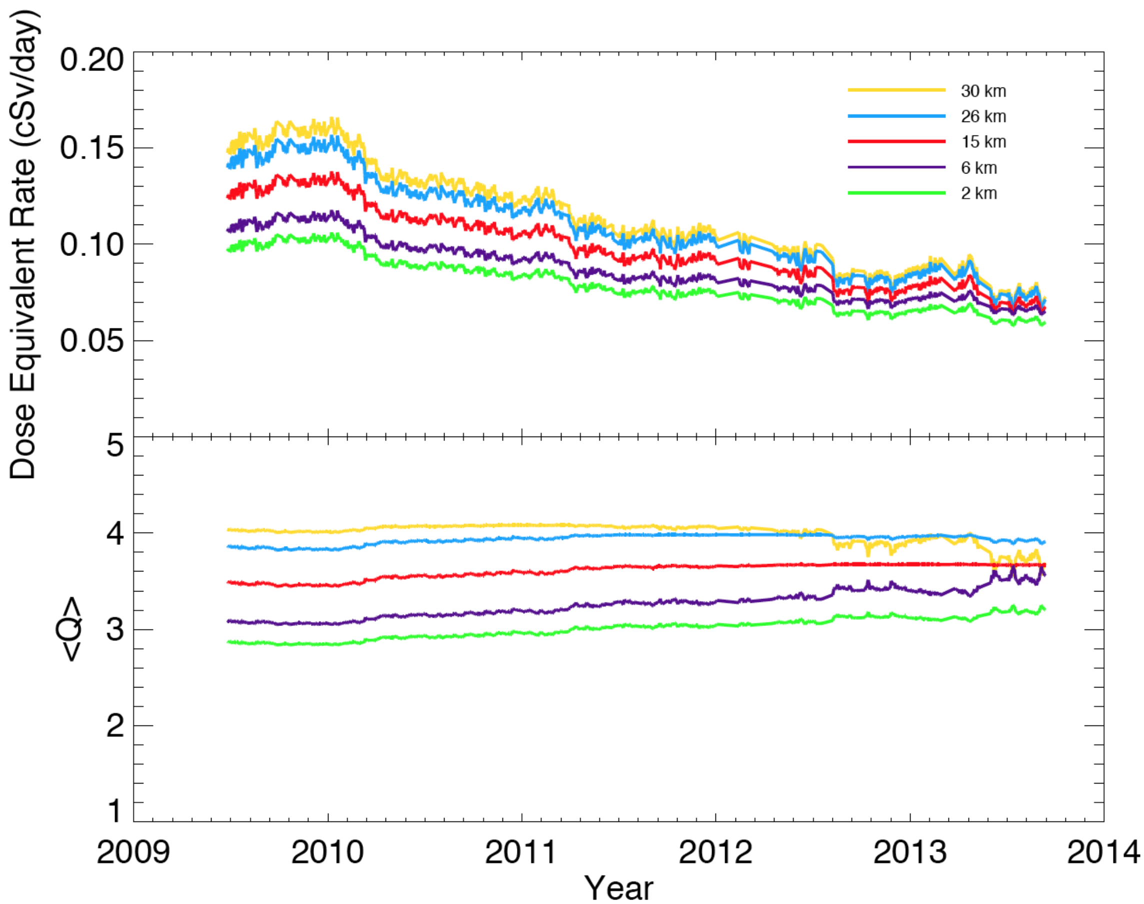

Figure 4. *Plot of GCR dose equivalent rates in the Martian atmosphere for various altitudes as well as the dose-weighted quality factor <Q>.. We see that, unlike for Earth, the dose equivalent rate values differ significantly from the dose rate values, being approximately a factor of four greater for the highest altitude and three for the lowest. We also see greater variation among the dose equivalent rates for different altitudes with the highest altitude being greater than the lowest by approximately 53% initially and 22% most recently.*

Relevant Publications

- Goelzer, M. L., Smith, C. W., Schwadron, N. A., and McCracken, K. G., An analysis of heliospheric magnetic field flux based on sunspot number from 1749 to today and prediction for the coming solar minimum, Journal of Geophysical Research (Space Physics), 118, 7525, 2013
- Schwadron, N. A., Smith, S., and Spence, H. E., The CRaTER Special Issue of Space Weather: Building the observational foundation to deduce biological effects of space radiation, Space Weather, 11, 47, 2013
- McComas, D. J., Angold, N., Elliott, H. A., Livadiotis, G., Schwadron, N. A., Skoug, R. M., and Smith, C. W., Weakest Solar Wind of the Space Age and the Current "Mini"

Solar Maximum, The Astrophysical Journal, 779, 2, 2013

- Smith, C. W., Schwadron, N. A., and DeForest, C. E., Decline and Recovery of the Interplanetary Magnetic Field during the Protracted Solar Minimum, The Astrophysical Journal, 775, 59, 2013
- Joyce, C., N. A. Schwadron, J. K. Wilson, H. E. Spence, J. C. Kasper, M. Golightly, J. B. Blake, L. W. Townsend, A. W. Case, E. Semones, S. Smith, and C. J. Zeitlin, Radiation Modeling in the Earth and Mars Atmospheres Using LRO/CRaTER with the EMMREM Module, *Space Weather Journal,* In Press, 2013a

II.2 C-SWEPA Progress in Modeling Solar Energetic particles

Solar energetic particles (SEPs) present significant acute hazards to human and robotic missions. The C-SWEPA project provides a unique coupling between MHD models and the energetic particle models, allowing fundamental capabilities to now-cast and predict the SEP events.

Significant progress has been made with PREDICCS (Predictions of Radiation from REleASE, EMMREM, and Data Incorporating the CRaTER, COSTEP and other SEP measurements, http://prediccs.sr.unh.edu), which is an online system that utilizes data from various satellites in conjunction with numerical models (C-SWEPA) to produce a near-real-time characterization of the radiation environment of the inner heliosphere. PREDICCS offers the community a valuable tool in forecasting events and improving risk assessment models for future space missions, providing up to date predictions for dose rate, dose equivalent rates and particle flux data at Earth, Moon and Mars. Joyce et al. [2013b] presented a comparison between lunar dose rates and accumulated doses predicted by the PREDICCS system with those measured by the Cosmic Ray Telescope for the Effects of Radiation (CRaTER) instrument aboard the Lunar Reconnaissance Orbiter (LRO) spacecraft during three major solar events in 2012 (Figure 5). We also plot the dose rate measured by the microdosimeter aboard LRO for comparison, as well as additional PREDICCS dose rates for different levels of shielding, which demonstrate how advanced knowledge of events may be used to reduce radiation exposure to astronauts. Joyce et al. [2013b] find that the dose rates and accumulated doses predicted by PREDICCS and measured by CRaTER during the three solar events are in good agreement and differ by at most 40 percent. From this, we conclude that PREDICCS offers a credible characterization of the lunar radiation environment. The Joyce et al. [2013b] study offers the first long-term validation of C-SWEPA radiation models using in-situ measurements and demonstrates how valuable PREDICCS should become in future efforts in risk assessment and in the study of radiation in the inner heliosphere. This study also demonstrates typical dose rates and accumulated doses associated with large solar events.

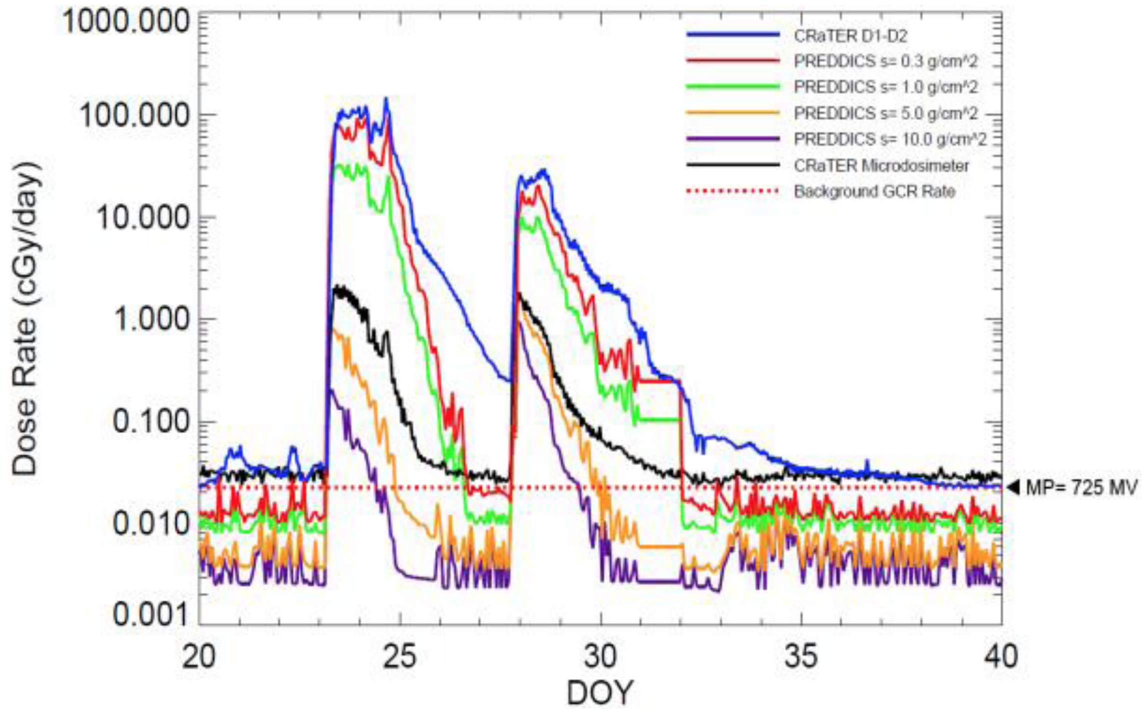

Figure 5. *Dose rates measured by CRaTER (blue) vs. those predicted by PREDICCS for various levels of shielding during the January 2012 solar event. The 0.3 g/cm2 shielded PREDICCS dose rate (red) offers the closest comparison to the level of shielding seen by CRaTER. Figure taken from Joyce et al., [2013b].*

Kozarev et al. (2013) coupled results from a detailed global three-dimensional MHD time-dependent CME simulation to a global proton acceleration and transport model, in order to study time-dependent effects of SEP acceleration between 1.8 and 8 solar radii in the 2005 May 13 CME. Kozarev et al. (2013) find that the source population is accelerated to at least 100 MeV, with distributions enhanced up to six orders of magnitude. Acceleration efficiency varies strongly along field lines probing different regions of the dynamically evolving CME, whose dynamics is influenced by the large-scale coronal magnetic field structure. We observe strong acceleration in sheath regions immediately behind the shock. Results from the Kozarev et al. (2013) study are shown in Figures 6-8.

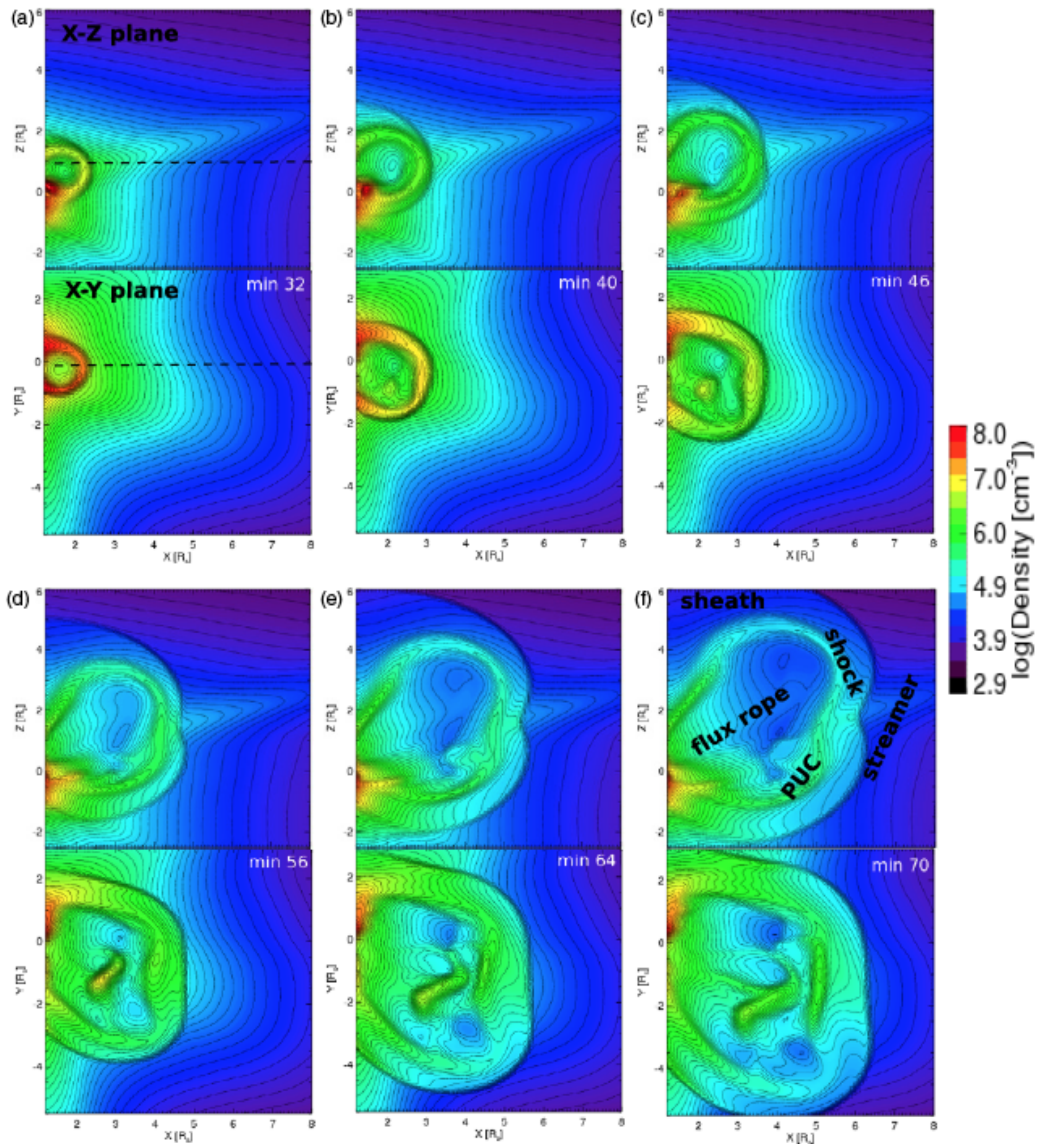

Figure 6. *X–Z and X–Y slices showing color and line contours of proton density for six snapshots of the CME simulation used in Kozarev et al. [2013]. The snapshots span about 38 minutes of simulation time. The larger structure is a coronal streamer.*

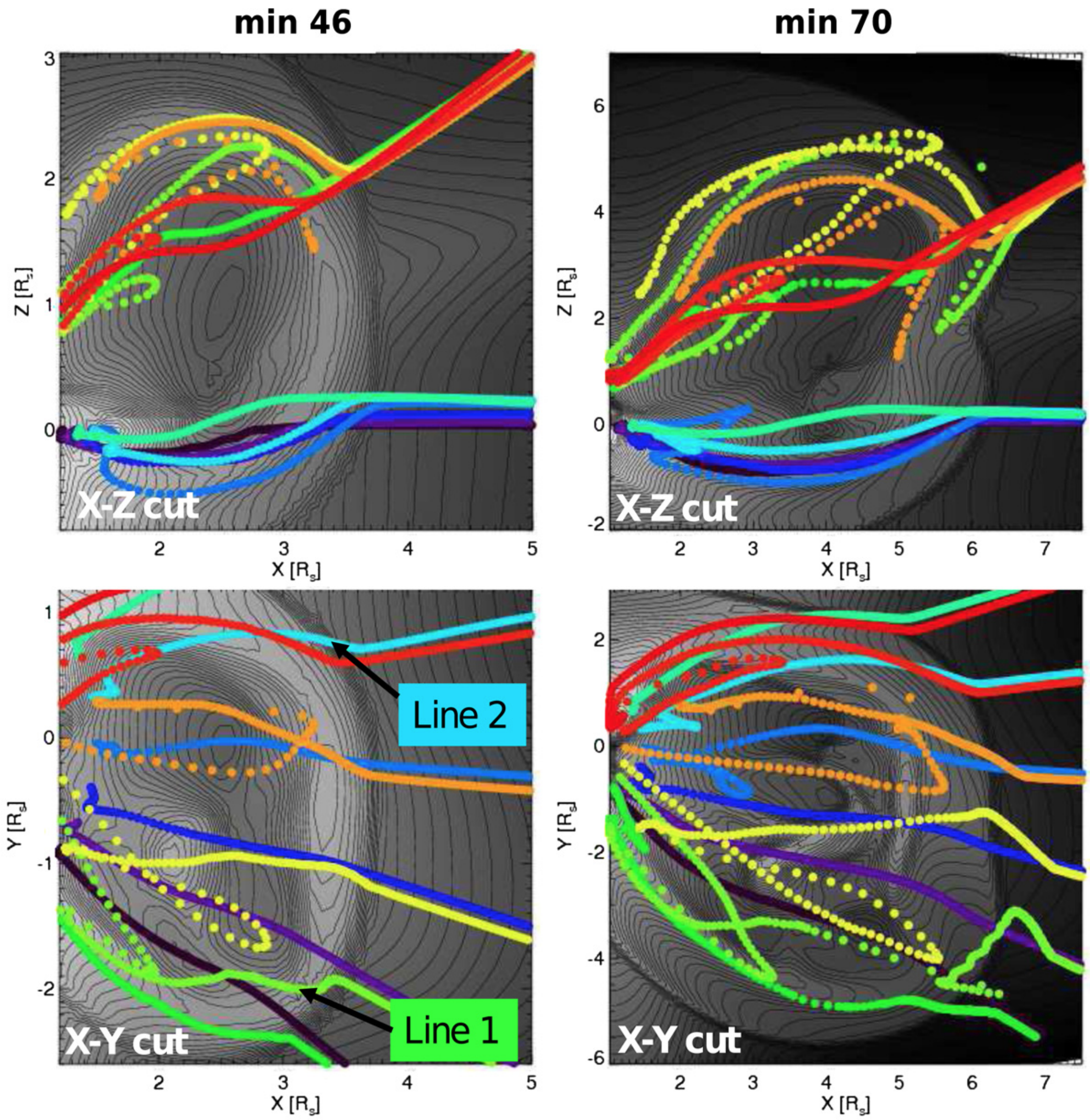

Figure 7. *Evolving CME distorts the C-SWEPA grid lines, as can be seen in these panels. The solar wind density is shown as grayscale density contours. Overlaid, color dots represent the grid node positions along individual field lines. The top and bottom panels show the X–Z and X–Y cuts for two times, similar to previous figures. The two lines marked "Line 1" and "Line 2" point to the two lines discussed later in this section. Figure taken from Kozarev et al., 2013.*

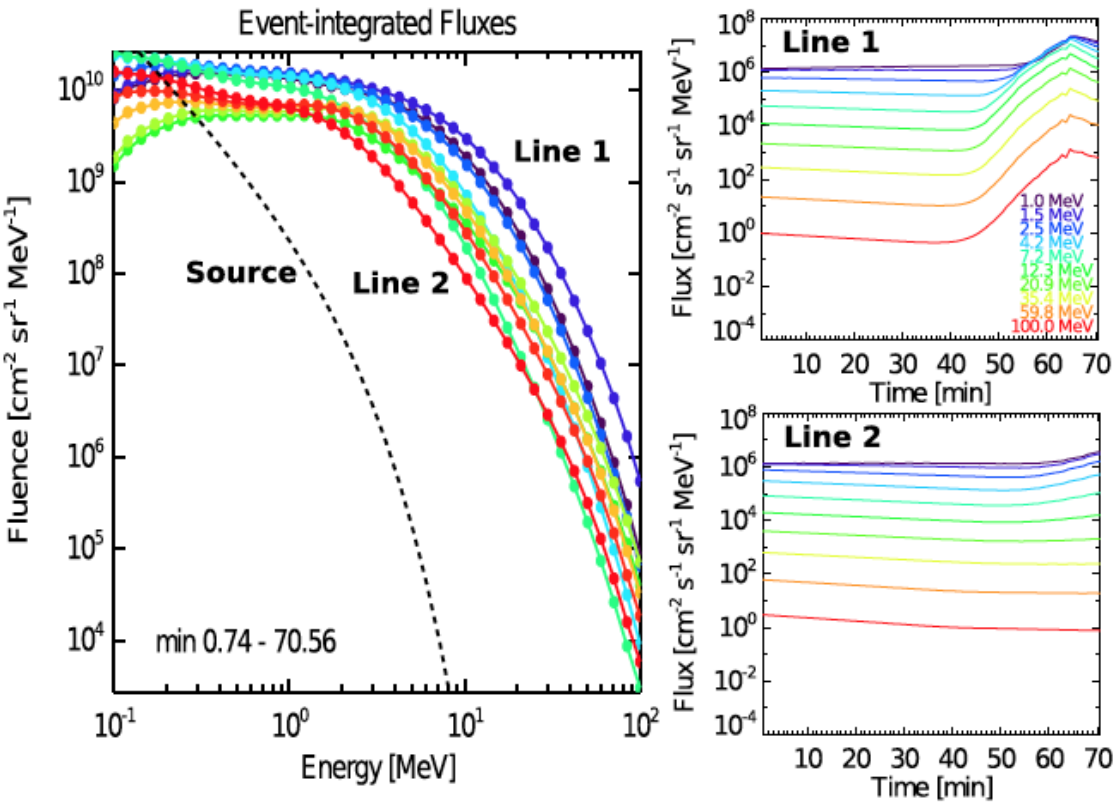

Figure 8. *Panel (a): event-integrated fluences for the 10 lines shown in Figure 5. Proton energy is on the X-axis; fluence is on the Y-axis. The dashed line represents the fluence at the model inner boundary (source). Panels (b) and (c): simulated flux, "measured" over time at a constant distance of ~8 RS on the two lines denoted in the bottom left panel of Figure 5 as Line 1 and Line 2, respectively. Time is on the X-axis; proton flux is on the Y-axis. Figure taken from Kozarev et al. [2013].*

The C-SWEPA team has (1) completed an analysis of the July 23, 2012 extreme CME event, including the acceleration of energetic particles; (2) completed a thermodynamic MHD relaxation run for the Bastille Day event; and (3) began preliminary simulations with an embedded spheromak field within our cone-model generator.

A suite of model solutions for the July 23, 2012 CME explored a variety of input parameters, including the shape, duration, amplitude, and speed of the main CME as well as whether or not a precursor CME was first launched. One promising candidate was chosen to provide the background plasma and magnetic field parameters to accelerate protons using the C-SWEPA code. The results suggest that the included particle acceleration mechanisms can more than adequately produce distributions like those observed. However, these 'coupled' simulations are limited in the sense that there is no feedback: the energetic particles are treated as test particles and the pressure is unbounded. For the July 23, 2012 event in particular, and, as pointed out by Russell et al. (2013), the intense flux of energetic particles may have substantially modified the plasma conditions. This level of coupling is significantly more challenging than the 'one-way' methodology currently employed. Nevertheless, it is likely to be a crucial component of any robust and accurate model in the future. Thus, we are developing plans to ultimately produce a coupled MHD/particle code that can self-consistently model the plasma, magnetic, and energetic particle properties of fast, and even extreme CMEs.

A thermodynamic MHD relaxation run was completed of the Bastille Day event corona with improved spatial resolution and inserted a pre-relaxed flux rope into the solution. The test, which was successful, was to assess whether the rope would remain coherent or transform into a sheared arcade. While a significant amount of magnetic energy was still released as the system adjusted to the inserted, strong-field flux rope, the rope now retains its coherence much better. Moreover, the improved resolution greatly improves the quality of synthetic satellite images in the sense that spurious oscillations and disturbances that we had previously seen in the images are now almost completely absent within the active region.

The C-SWEPA team further developed an analytic description of the modified Titov-Demoullin (TDm) model. We were able to eliminate the current concentrations surrounding the symmetry axis of the TDm current ring, allowing us to study tilted (with respect to the vertical direction) flux rope configurations without introducing unphysical currents into the domain. We are currently running test simulations of this updated version.

To address the limitation that current cone model simulations cannot capture any of the magnetic structure within ICMEs, we developed a simple prescription of a spheromak magnetic field that can be inserted within a cone model ejecta. Although the dynamics of the eruption are still primarily controlled by the plasma properties of the ejecta (speed and density primarily), initial tests suggest that even a modest magnetic field modifies the profiles of the disturbance at 1 AU. We are in the process of investigating these results in more detail, and, in particular, assessng the effects of different field strengths within the ejecta.

Figures 9 – 14 exemplify results of recent model runs that explore the effects of CMEs on solar energetic particles. These results are currently being incorporated in several draft manuscripts in preparation.

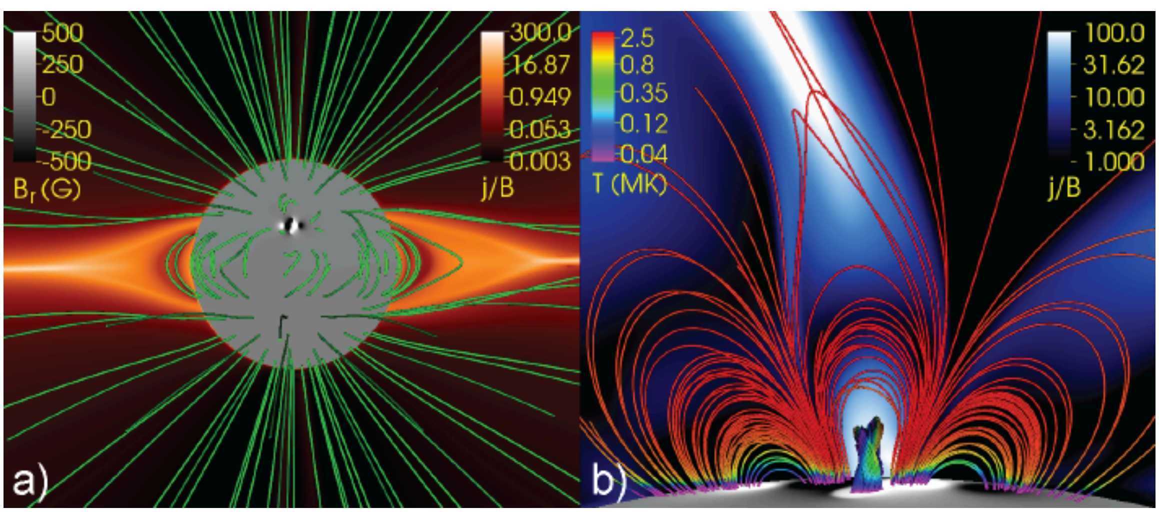

Figure 9. *[Titov et al., 2013] Magnetic field configuration after flux rope insertion and subsequent relaxation. active region located in the northern hemisphere. b): View on the active region. Field lines are colored by temperature. Cold (and dense) flux rope core is visible in the center. The streamer is seen overlying the active region.*

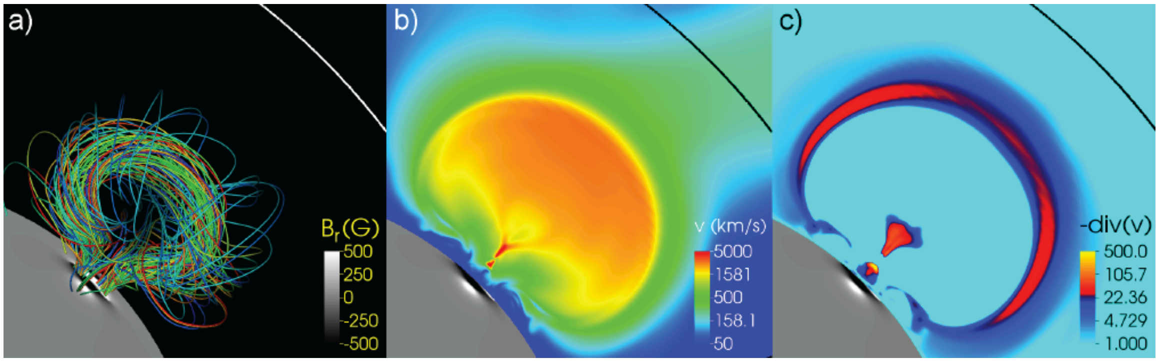

Figure 10. *Modified version of the flux rope model by Titov & Demoulin (1999) above the central polarity inversion line of an active region. Active region and flux rope total unsigned flux of 7.5 x 10^{22} Mx. Maximum radial-field strength of 1070 G at the photospheric level. [from Gorby et al., 2013]*

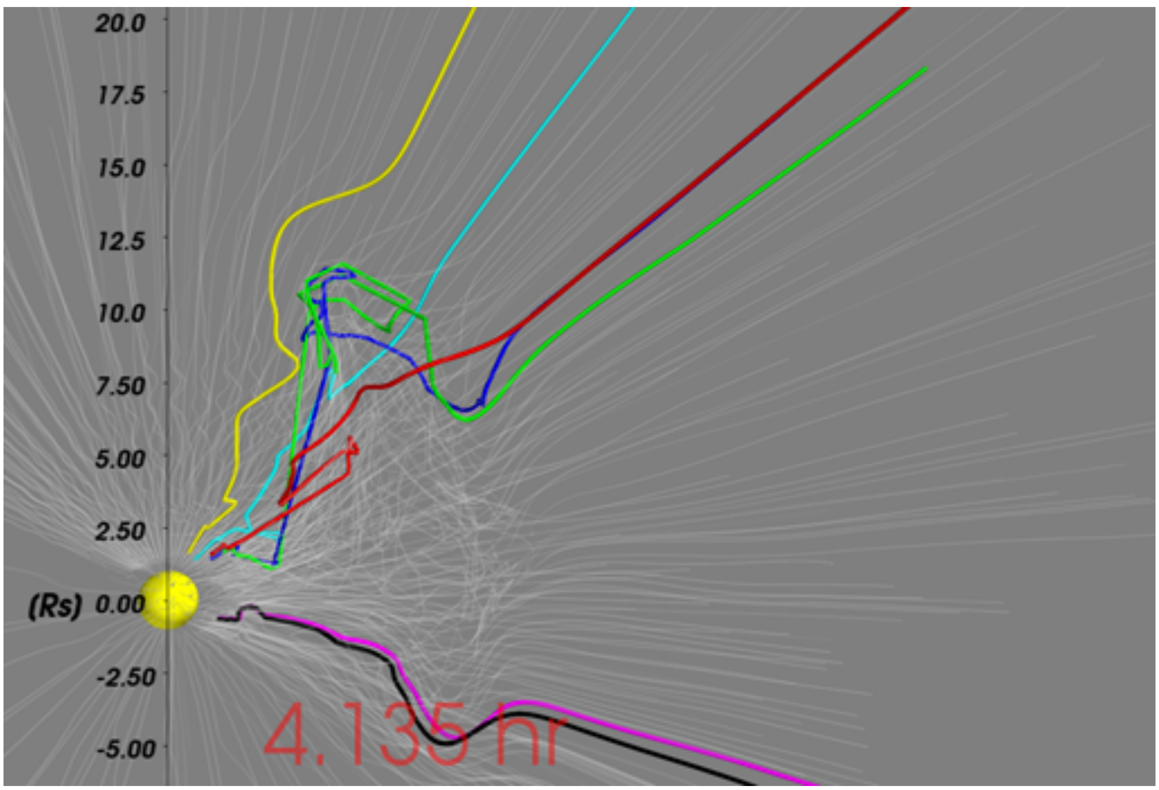

Figure 11. *Energetic particles are accelerated over a broad latitudinal and longitudinal spread from the CME released following destabilization shown in Figure 10. The colored magnetic field lines show strong distortions by the plasma flow. [from Gorby et al., 2013]*

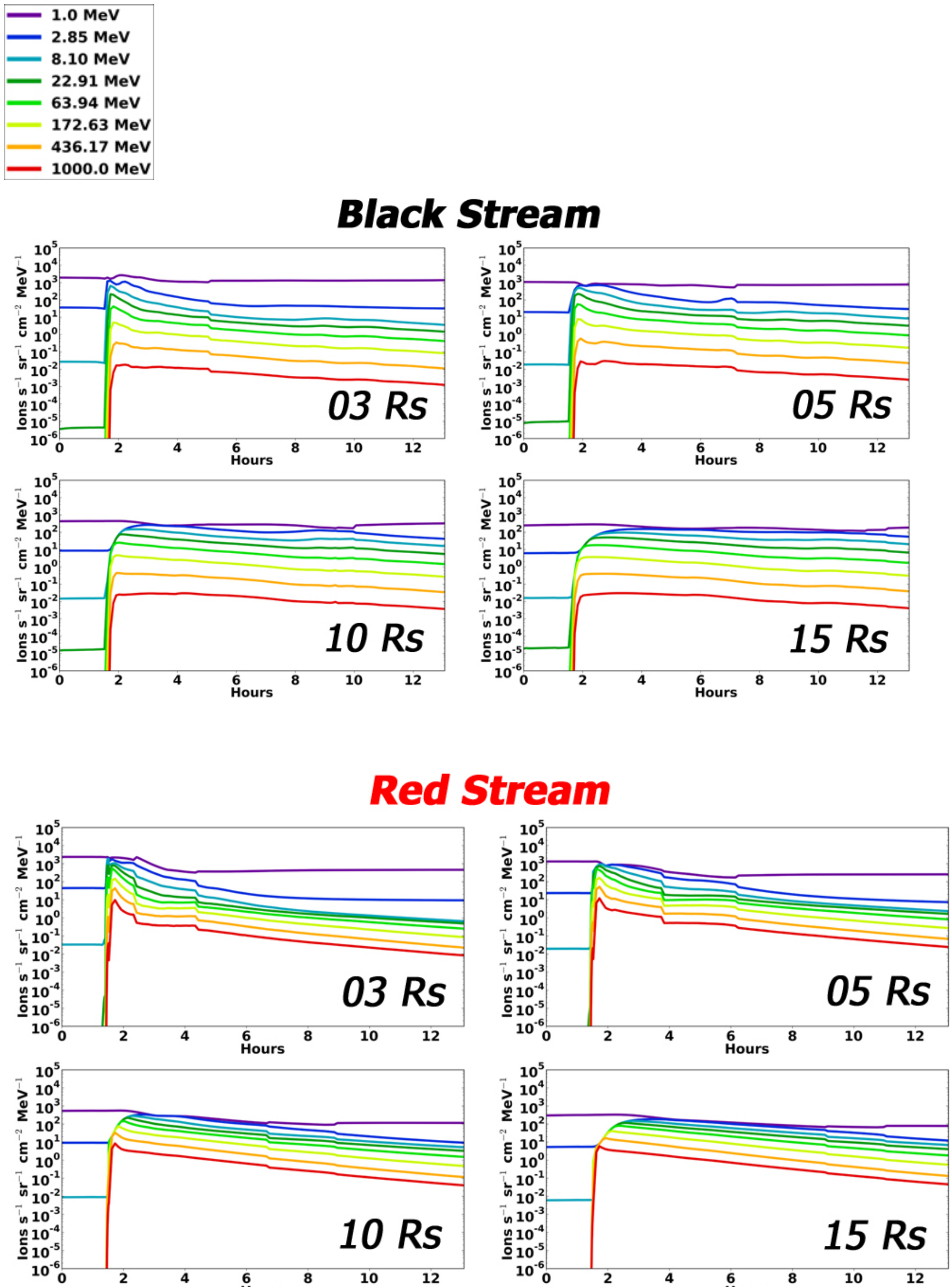

Figure 12. *The CME from figures 10 and 11 causes particle acceleration up to GeV energies. Shown here are the time-dependent histories of energetic particles at 3, 5, 10 and 15 solar radii along the Black and Red Streamlines shown in Figure 11. [from Gorby et al., 2013]*

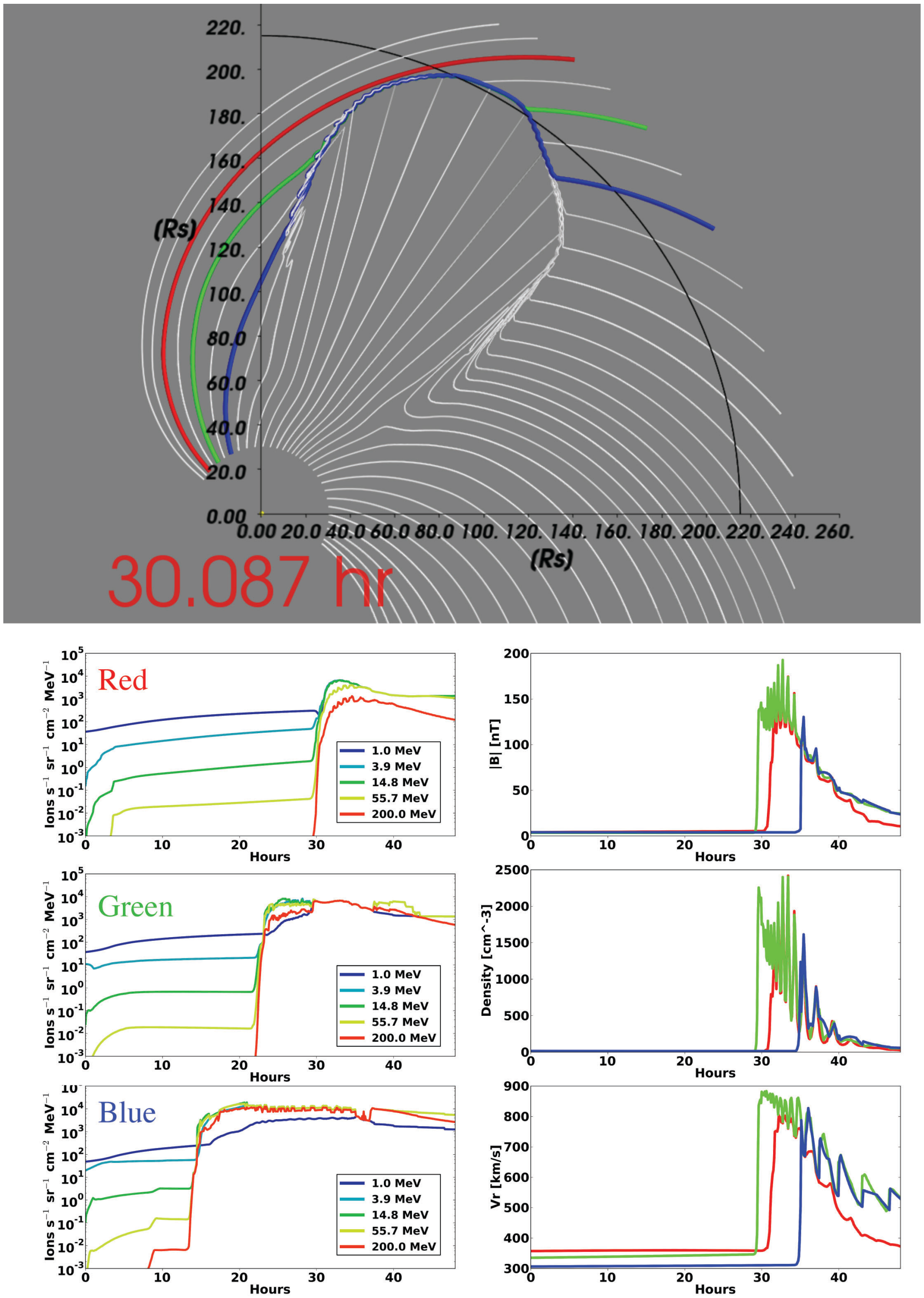

Figure 13. *C-SWEPA models solve for the energetic charged particle distributions along and across magnetic field lines, from Kev to Gev energies. The code produces time histories of the particle distribution functions at various pitch angles, energies, and locations within the heliosphere. The red/green/blue traces shown here represent fluxes associated with the*

west/center/east of the ICME, that is, two at the flanks and one near the nose. [From Riley et al., 2013]

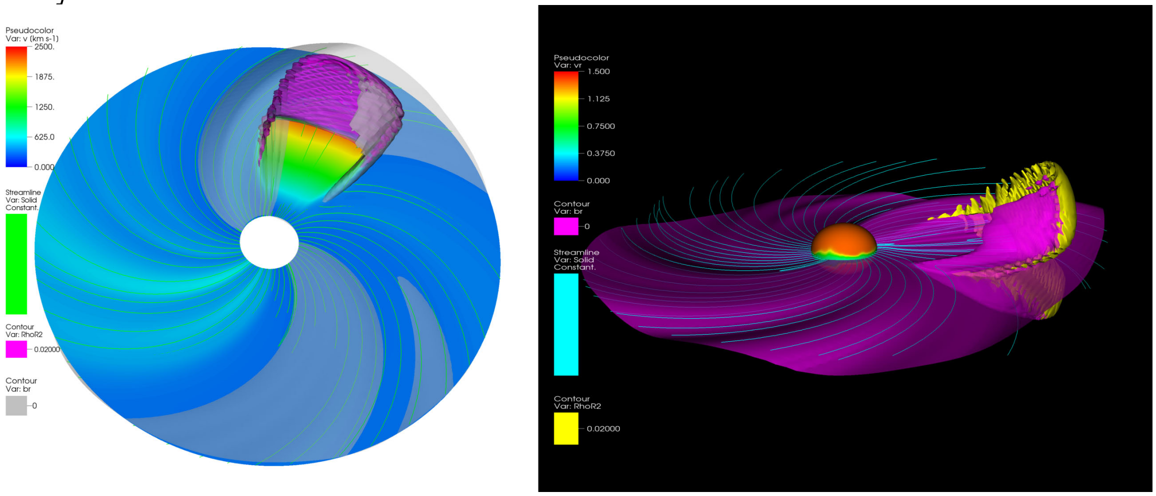

Figure 14. *Two 3-D views of ICME (simulation 15) as it approaches 1 AU. The legends to the left of each panel indicate what parameters are being displayed. A selection of interplanetary magnetic field lines are also shown [From Riley et al., 2013].*

Relevant Publications:

- Valori et al., "Initiation of Coronal Mass Ejections by Sunspot Rotation", Proceedings IAU Symposium No. 300, 2013.
- Torok et al., "The Evolution of Writhe in Kink-Unstable Flux Ropes and Erupting Filaments", submitted to PPCF (Plasma Physics and Controlled Fusion).
- Torok et al., "Distribution of Electric Currents in Solar Active Regions", submitted to ApJ Letters
- Lionello et al., "Magnetohydrodynamic Simulations of Interplanetary Coronal Mass Ejections", ApJ 777, 76 (2013).
- Leake et al., "Simulations of Emerging Magnetic Flux. I: The Formation of Stable Coronal Flux Ropes", ApJ 778, 99 (2013).
- Lugaz, N., Farrugia, C. J., Manchester, W. B., IV, and Schwadron, N., The Interaction of Two Coronal Mass Ejections: Influence of Relative Orientation, The Astrophysical Journal, 778, 20, 2013
- Joyce, C. J., Schwadron, N. A., Wilson, J. K., Spence, H. E., Kasper, J. C., Golightly, M., Blake, J. B., Mazur, J., Townsend, L. W., Case, A. W., Semones, E., Smith, S., and Zeitlin, C. J., Validation of PREDICCS using LRO/CRaTER observations during three major solar events in 2012, Space Weather, 11, 350, 2013
- Kozarev, K. A., Evans, R. M., Schwadron, N. A., Dayeh, M. A., Opher, M., Korreck, K.

E., and van der Holst, B., Global Numerical Modeling of Energetic Proton Acceleration in a Coronal Mass Ejection Traveling through the Solar Corona, The Astrophysical Journal, 778, 43, 2013

Relevant Presentations

- M Gorby, N A Schwadron, M A Lee, A C Booth, H E Spence, T Torok, C Downs, R Lionello, J Linker, V S Titov, Z Mikic, P Riley, M I Desai, M A Dayeh, K A Kozarev, Particle Acceleration in the Low Corona Over Broad Longitudes: Coupling Between 3D Magnetohydrodynamic and Energetic Particle Models, Fall AGU, 2013
- P Riley, M Ben-Nun, R Lionello, C Downs, T Török, J Linker, Z Mikic, N Schwadron and M Gorby, Understanding the Evolution of the July 23, 2012 Extreme ICME: Global Modeling and Comparison with Observations, Fall AGU, 2013
- Joyce, C. J., Blake, J. B., Case, A. W., Golightly, M., Kasper, J. C., Mazur, J., Schwadron, N. A., Semones, E., Smith, S., Spence, H. E., Townsend, L. W., Wilson, J. K., and Zeitlin, C. J., Validation of PREDICCS Using LRO/CRaTER Observations During Three Major Solar Events in 2012, Lunar and Planetary Institute Science Conference Abstracts, 44, 2707, 2013

II.3 Survey of Spectral Properties of SEP events from solar cycles 23 and 24

Members of the C-SWEPA team have identified all SEP events observed at ACE and Wind during solar cycles 23 and 24. We have obtained the energy spectra of ~0.1–100 MeV/nucleon heavy ions for 11 species H, He, C, N, O, Ne, Mg, Si, S, Ca, and Fe during each of these events using ACE/ULEIS and ACE/SIS data. We have also performed spectral fits to these data to calculate the break-point energies or the energy at which each species rolls-over (departs from a single power-law). An example of these types of energy spectral breaks during an ESP event and how they are related to existing theoretical ideas is shown in Figure 15.

Recent particle acceleration models have taken account of the complex interplay between the injection of compound suprathermal seed populations and the time-dependent evolution and spatial curvature of IP shocks (e.g., Tylka & Lee 2006; Li et al., 2009). To date such models have simulated the time-histories of a variety of heavy ion species during individual SEP events (e.g., Ng et al., 2003; Li et al., 2005) and constructed event-integrated or event-averaged heavy ion spectra over a broad energy range that were then compared with SEP observations near Earth (e.g., Mewaldt et al., 2007; Mason et al., 2013).

For instance, Tylka & Lee (2006) neglected transport effects and used an analytical approach to model the event-integrated abundances of heavy ions and the energy-dependence of Fe/O in two large SEP events. They assumed that the heavy ion differential intensity spectra in individual SEP events can be fitted with power-laws modulated by exponential roll-overs of the form $J_X(E,\theta_{Bn}) = C_X E^{-\gamma} \exp(-E/E_{0X})$, where J_X is the differential intensity of species X at energy E measured in MeV/nucleon, C_X is the normalization constant, γ is the power-law index, and E_{0X} is the e-folding energy, i.e., the energy at which the spectrum starts to roll-over or deviate from a pure power-law (e.g., Jones & Ellison 1991). In this model, the behavior of the heavy ion abundances and the energy-dependence of Fe/O arise from the relative amount of solar wind-like or flare-like material in the suprathermal seed population; the dominant material being determined by the shock's θ_{Bn} or the injection threshold. In the Tylka & Lee model, these factors result in producing roll-overs or breaks in the event-integrated heavy ion spectra that depend on the ion's Q/M ratio and the shock's θ_{Bn} as follows: $E_{0X}/E_{0H} \equiv (Q_X/M_X)^{\delta}(\sec\theta_{Bn})^{2/(2\gamma-1)}$. Here E_{0H} is the proton roll-over energy, the exponent δ arises from the Q/M-dependence of the parallel mean free path $\lambda_{//} \propto (Mv/Q)^s$ and is given by $\delta = 2s/(s+1)$ when the parallel diffusion coefficients $\kappa_{//}$ for different species are equal (see e.g., Cohen et al., 2005; Li et al., 2009). For simplicity, Tylka & Lee (2006) assumed that δ~1, i.e., s~1 and found good agreement between the event-integrated abundances of heavy ions and the energy-dependence of Fe/O in two large SEP events.

Li et al. (2009) took account of transport effects and used the equal diffusion coefficient condition to obtain a more general model in which δ has values ranging from ~0.2 for perpendicular shocks to ~2 for parallel shocks, with values in between corresponding to oblique shocks. In this model, the strongest Q/M-dependence in the spectral roll-overs occur at parallel shocks, while the weakest occurs at perpendicular shocks. Note that Mewaldt et al. (2007) obtained a value of δ ~1.75 for the October 2003 ESP/SEP event.

Figure 15 shows a preliminary analysis for an IP shock event from the Desai et al. (2003;

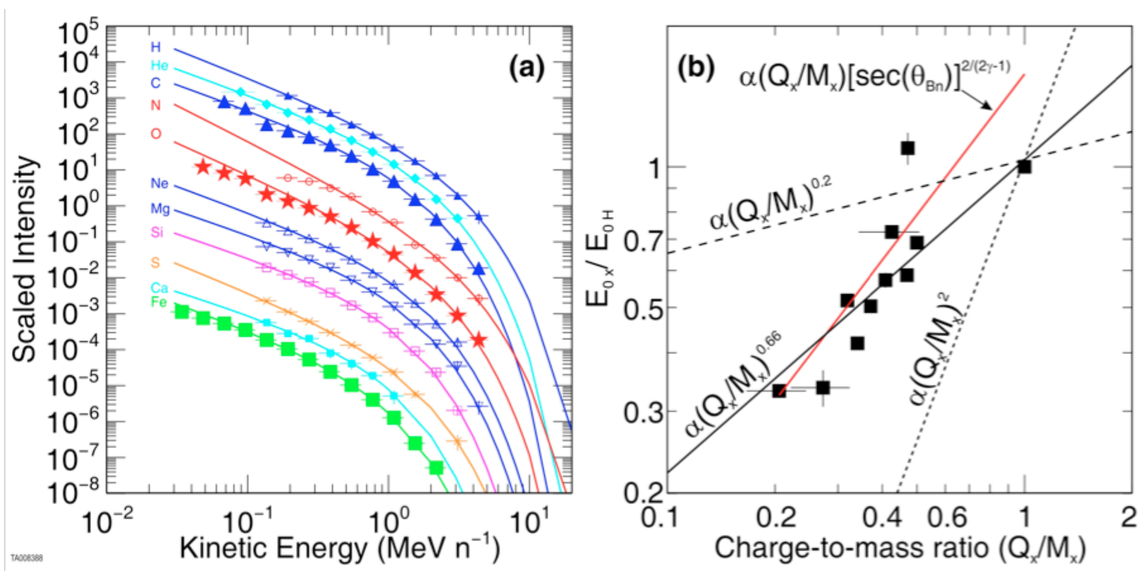

Figure 15: *(a) Heavy ion spectra and fits (see text for details) for the IP shock-associated ESP event on June 26, 1999. (b) Scatterplots of e-folding energies E_{0X}/E_{0H} for species X vs. the ion's Q/M ratio. The dashed and dotted black lines represent $E_{0X}/E_{0H} \propto (Q_X/M_X)^{\delta}$ for δ=0.2 and δ=2, corresponding to perpendicular and parallel shocks (after Li et al., 2009). Red line: Fits to $E_{0X}/E_{0H} \equiv (Q_X/M_X)(\sec\theta_{Bn})^{2/(2\gamma-1)}$ assuming a constant γ=1.45 for all species (after Tylka & Lee 2006); black line: least squares fit of the form $E_{0X}/E_{0H} \propto (Q_X/M_X)^{0.66}$. The black line is a reasonable representation of the Q/M-dependence for this event, in agreement with the Li et al. (2009) simulations for an oblique IP shock.*

2004) surveys, which had θ_{Bn}≈55°±2° and also exhibited a strong energy dependence in the Fe/O ratio. The H-Fe differential intensity spectra in Figure 15a are fitted by the Jones & Ellison expression, with free parameters C_X, γ_X, and E_{0X}. Figure 15b shows the ratio of roll-over or e-folding energies E_{0X}/E_{0H} vs. the Q/M ratio of each species *X*. The solid black line shows a fit to the data with $E_{0X}/E_{0H} \propto (Q_X/M_X)^{\delta}$ with δ~0.67±0.08; dashed black lines show the Q/M-dependence with δ~0.2 and δ~2. The red line shows a fit of the form $E_{0X}/E_{0H} \equiv (Q_X/M_X)(\sec\theta_{Bn})^{2/(2\gamma-1)}$ assuming a constant *γ~1.45* for all species (after Tylka & Lee 2006). Figure 15b shows that the red line with δ~1 and the solid black line with δ~0.66 are reasonable representations of the observed Q/M-dependence of the spectral roll-overs, and are therefore in apparent agreement with model expectations of injection and acceleration of solar-wind like material at an oblique shock.

Relevant Publications:

- Mason, G. M., M. I. Desai, R. A. Mewaldt, and C. M. S. Cohen, "Particle Acceleration in the Heliosphere," in American Institute of Physics Conference Proceedings, vol., 1516, pp 117-120, 2013

Relevant Presentations

- Desai, M. I., D. J. McComas, E. R. Christian, A. C. Cummings, J. Giacalone, M. E. Hill, S. M. Krimigis, S. A. Livi, R. L. McNutt, R. A. Mewaldt, D. G. Mitchell, W. H. Matthaeus, E. C. Roelof, T. T. von Rosenvinge, N. A. Schwadron, E. C. Stone, M. M. Velli, and M. E. Wiedenbeck, "Suprathermal and Solar Energetic Particles: Key Questions for Solar Probe Plus," Invited Talk (30 minutes), presented at the 1st Solar Probe Plus Workshop, Pasadena, March 26-29, 2013

II.4 Data Sharing and Products

The database of Wind IP shocks and Rankine solutions contributed by Mike Stevens (SAO/CfA) is alive and well, and up to date through July of this year at http://www.cfa.harvard.edu/shocks/wi_data/. The data set is an extremely valuable resource for the heliopshysics community since it quantifies the strength, frequency and detailed behavior of interplanetary shocks. Modeling using the C-SWEPA framework is now being extended to 1 AU and comparison with the IP shock dataset is increasingly valuable as a means of validating simulation results.

NASA's Virtual Energetic Particle Observatory (VEPO) provides enhanced access to energetic particle data sets of strong interest to C-SWEPA for comparison of time intensities and variously-averaged flux spectra from still-operational experiments on ACE, Stereo-A/B, Wind, SOHO, and GOES. Archival data are also available from Ulysses, IMP-8, Pioneer 10 & 11, and Voyager 1 &2. Fluxes and spectra can be compared from various sources for omnidirectional protons, helium, and heavier ions. The most recent addition includes directional sectored fluxes and spectra. VEPO enables C-SWEPA and other users to see selected fluxes and spectra averaged over user-selected time intervals. VEPO is very useful for comparison of evolving flux spectra from solar energetic particle (SEP) events as observed by multiple spacecraft sources in the heliosphere. A key motivation of these VEPO services is to enable cross-comparison of spectra from different sensors on the same spacecraft and from different locations to check flux calibrations. This function becomes maximally useful in the case of inner heliospheric "reservoir events" in which spatial gradients vanish during the decay phases of some SEP events. VEPO is now planning to add such services for energetic electron data products.

NASA funding for VEPO is continuing through FY14 and may continue at levels TBD into the future. C-SWEPA Collaborator John Cooper at NASA Goddard Space Flight Center is the Principal Investigator for VEPO. The web site is accessible at vepo.gsfc.nasa.gov.

III. Summary.

The major milestone for year 1 involves procuring hardware and the modeling of a single event out to 1 AU. The team is in the process of writing up two separate papers in which models of separate CMEs and energetic particles out beyond 1 AU are being performed. The C-SWEPA team has exceeded the milestone in the modeling of SEP events, CMEs and the analysis of observations in the remarkable mini-maximum of solar cycle 24.

The team is now gearing up for more extensive analysis of model results and comparison with observations. An important unanticipated result is the significance of energetic particle pressure even in the low corona. As detailed in the report, this result will require a stronger coupling between energetic particle and MHD models than previously planned. This activity in coupling these powerful models is both an ambitious goal, and one that can be uniquely achieved by the C-SWEPA team.

The C-SWEPA team has been extremely productive over the course of 2013 with 13 outstanding publications covering a broad array of topics from the modeling of CMEs to the effects of energetic particles and galactic cosmic rays. The team has hit the ground running and we anticipate another highly productive year.